

Role of entropy barriers for diffusion in the periodic potential

O. M. Braun*

Institute of Physics, National Ukrainian Academy of Sciences, 03650 Kiev, Ukraine

$$D = D_f G(h), \quad (2)$$

Diffusion of a particle in the N -dimensional external potential which is periodic in one dimension and unbounded in the other $N - 1$ dimensions is investigated. We find an analytical expression for the overdamped diffusion and study numerically the cases of moderate and low damping. We show that in the underdamped limit, the multi-dimensional effects lead to reduction (comparing with the one-dimensional motion) of jump lengths between subsequent trapping of the atom in bottoms of the external periodic potential. As application we consider the diffusion of a dimer adsorbed on the crystal surface.

I. INTRODUCTION

A variety phenomena in physics and other fields can be modeled as Brownian motion in an external periodic potential [1–3]. One of particular example, the surface diffusion of atoms or small clusters, is of great fundamental and technological interest [4]. During crystal growth the deposited atoms diffuse over the surface until they become incorporated in the lattice. On the semiconductor Si(100) or Ge(100) surface, most of the deposited Si or Ge atoms combine to form dimers, and the diffusion of such dimers has recently been studied experimentally by a scanning tunneling microscope [5]. Moreover, atoms adsorbed on metal surfaces in some cases form closely packed islands which diffuse as a whole [6,7].

Theoretically the problem of diffusion can be described by a Langevin equation for the atom(s) or, equivalently, a Fokker-Planck-Kramers equation for the distribution function in the phase space [1,2]. In the trivial case of Brownian motion without the external potential, the diffusion coefficient is equal to $D = D_f \equiv k_B T / m \eta$, where k_B is the Boltzmann constant, T is the temperature, m is the particle mass, and η is the viscous damping coefficient which models the energy exchange with the substrate (thermostat). For a single atom in the one-dimensional (1D) sinusoidal external (substrate) potential the value of diffusion coefficient is well known as summarized in the Risken monograph [1]. Exact results exist for the overdamped (Smoluchowski) case, $\eta \rightarrow \infty$, when [8]

$$D = D_f I_0^{-2}(h), \quad (1)$$

where $h \equiv \varepsilon / 2k_B T$, ε is the (total) height of the substrate potential and $I_0(h)$ is the modified Bessel function, and in the underdamped limit, $\eta \rightarrow 0$, when [1]

where $G(h) = (h/2\pi)^{1/2} e^h I_0^{-1}(h) J(h)$, $J(h) = \int_0^1 du u^{-3/2} e^{-2h/u} \mathbf{E}^{-1}(u)$, and $\mathbf{E}(u)$ is the complete elliptic integral of second kind. At low temperatures, $k_B T \ll \varepsilon$, both expressions (1) and (2) take the Arrhenius form, $D = \tilde{D} A$ with $A = \exp(-\varepsilon/k_B T)$ and $\tilde{D} \approx \omega_0^2 a^2 / 2\pi \eta$ in the high-friction case [here a is the period of the substrate potential and $\omega_0 = (2\pi/a)(\varepsilon/2m)^{1/2}$ is the frequency of oscillation at its minimum], and $\tilde{D} \approx \pi D_f / 2$ in the low-friction limit. In a general case the diffusion coefficient can be found numerically with practically any desired accuracy by the matrix continued-fraction-expansion method [1].

At low temperatures, $k_B T \ll \varepsilon$, when the diffusion proceeds by uncorrelated thermally activated jumps over the barrier from one minimum of the external potential to another, the diffusion coefficient may be presented as $D = RA \langle \lambda^2 \rangle$, where RA is the rate of escape from a minimum of the external potential and $\langle \lambda^2 \rangle$ is the mean-square jump length. For a moderate or large damping, $\eta \gtrsim \omega_0$, when only jumps for one period a of the external potential are possible, one should take $\lambda = a$ and $R = R_{\text{TST}} B(\eta)$, where $R_{\text{TST}} = \omega_0 / 2\pi$ is the escape rate given by the transition state theory (TST) [2,9], and the factor $B(\eta) = (z^2 + 1)^{1/2} - z$ with $z = \eta / 2\omega_s$ provides an interpolation between the TST and overdamped limits as was found by Kramers [10] [here ω_s is the ‘‘saddle’’ frequency at the saddle point $x = x_s$, near which the external potential has the form $V(x) \approx \varepsilon - \frac{1}{2} m \omega_s^2 (x - x_s)^2$; for the sinusoidal potential $\omega_s = \omega_0$]. The underdamped limit, $\eta \ll \omega_0$, is qualitatively different: in this case $R \approx 2\eta \varepsilon / \pi k_B T \propto \eta$ as was found firstly by Kramers [10], but the average jump length diverges as $\lambda \propto \eta^{-1}$, thus this again leads to the dependence $R \lambda^2 \propto \eta^{-1}$ similarly to the overdamped case. The occurrence of long jumps, $\lambda > a$, has been observed in a number of experiments on surface diffusion [4,11]. The interval from low to moderate friction is covered by the Mel’nikov-Meshkov formula [12]

$$R_{\text{MM}} \approx R_{\text{TST}} \exp \left(\frac{1}{\pi} \int_0^\infty du \frac{\ln \left[1 - e^{-\Delta(u^2 + \frac{1}{4})} \right]}{u^2 + \frac{1}{4}} \right), \quad (3)$$

where $\Delta = 8h\eta/\omega_0$. Thus, the whole interval of frictions may be described by the interpolation formula $R \approx R_{\text{MM}} B(\eta)$, which was checked numerically in [13]. Combining this expression for R with the numerically calculated values of D , one can find the distribution of

jump lengths [14]. Note that the widely used TST expression $D \approx R_{\text{TST}} A a^2$, where the diffusion coefficient does not depend on the damping coefficient, operates in fact for a narrow interval of frictions close to the point $\eta \sim \omega_0$ only (which, fortunately, often corresponds to experimental situations).

Although the described above results for one-dimensional diffusion are very important and often lead to reasonable estimations for experimentally measured diffusion coefficients, in real systems the motion always takes place in a $N > 1$ configurational space. Indeed, even for diffusion of a single atom adsorbed on a crystal surface $N = 2$ at least. Besides, the diffusing object may have internal degrees of freedom. Multi-dimensional effects modify both the escape rate R and the jump length λ . The escape rate can be presented as $R = R_{1\text{D}} F$, where the coefficient F is known as the “entropy factor” [15]. The value of F can be found with the help of transition state theory [9] which yields $F \approx (\prod_i \omega_{0,i}) / (\prod_i \omega_{s,i})$, where $\omega_{0,i}$ are the frequencies at the minimum and $\omega_{s,i}$ are the “saddle” frequencies for all degrees of freedom i except the given one along the diffusion path. In this approach F can be interpreted as $F = \exp(\Delta S/k_B)$, where ΔS is the difference in entropy of the saddle and minimum-energy configurations. The entropy factor is often used to explain the “compensation effect” [4], when at experiment one observes that a decrease of the activation energy (calculated as a slope of the Arrhenius plot of $\ln D$ versus T^{-1}) is compensated by decreasing of the prefactor. As for the jump length, while for $\eta \gtrsim \omega_0$ it still is given by $\lambda = a$, in the underdamped limit it is modified qualitatively comparing with the one-dimensional case. In the multi-dimensional space, the path connecting adjoining minima of the external potential may not coincide with the direction of easy crossing at the saddle point. Therefore, the probability of deactivation during long jumps is enhanced, leading to the reduction of jump length, $\lambda < \lambda_{1\text{D}}$ [16–18]. In particular, for the 2D-periodic substrate potential with the square symmetry it was found numerically [18] that $D \propto \eta^{-0.5}$ which gives $\lambda \propto \eta^{-0.75}$.

The multi-dimensional effects are also important in diffusion of molecules or small clusters: even for diffusion in the 1D periodic potential (e.g., along “channels” on furrowed or stepped surfaces) one has for the dimer diffusion $N = 2$ at least. Diffusion of the dimer was studied numerically by Vollmer [19] with the help of matrix continued-fraction-expansion technique. The adiabatically slow motion of a linear molecule in the 1D sinusoidal potential was analyzed in [20], where the adiabatic trajectory was found for a general case. This allowed to find the activation barriers and the minimum-energy and saddle-state frequencies and then to estimate the diffusion coefficient.

The aim of the present paper is to study the multi-dimensional effects in diffusion processes. We consider two typical examples: motion of a single atom in a “channel” which is periodic in one dimension and parabolic in others, and diffusion of a dimer (two-atomic molecule)

in the 1D sinusoidal potential. We find an analytical solution for the overdamped case and analyze numerically the dependence of diffusion coefficient on the damping constant η . The numerical results were obtained with the Verlet algorithm by calculating the trajectory $x(t)$ and then splitting it into N_{tr} pieces, each of the time duration τ . The diffusion coefficient was then calculated as $D = \langle \Delta x^2 \rangle / 2\tau$.

The paper is organized as follows. In Sec. II we obtain the analytical expression for the diffusion coefficient in the overdamped limit. In Sec. III A we analyze the case of pure entropic barriers. In Sec. III B the activated diffusion of a single atom is studied. In Sec. III C the diffusion of a dimer is described. Finally, Sec. IV concludes the paper.

II. OVERDAMPED LIMIT

Consider a particle moving in the N -dimensional external potential $V_N(x, y_1, \dots, y_{N-1})$ which is periodic in the x direction,

$$V_N(x + a, \dots) = V_N(x, \dots), \quad (4)$$

and grows unboundedly in the other $N - 1$ dimensions,

$$V_N(x, y_1, \dots, y_{N-1}) \rightarrow \frac{1}{2} \omega_i^2(x) y_i^2 \quad \text{if } y_i \rightarrow \pm\infty, \quad (5)$$

where $\omega_i(x) > 0$ for all x .

With presence of a viscous friction, the particle motion should be diffusive at long-time scale. The diffusion coefficient D can be found with the Einstein relation $D = T\mu$, where the mobility μ describes the proportionality between the linear current j and the infinitesimal external dc force f which causes this current, $j = \mu f$. Therefore, we have to consider the particle motion in the external potential

$$V_f(x, y_1, \dots, y_{N-1}) = V_N - fx, \quad (6)$$

and then take the limit $f \rightarrow 0$.

In the overdamped case, when the friction coefficient η is much larger than the characteristic system frequencies, the motion of the particle is described by the Smoluchowski equation

$$T \frac{\partial W}{\partial t} + \vec{\nabla} \cdot \vec{J} = 0, \quad \vec{J} = -\eta^{-1} (W \vec{\nabla} V_f + T \vec{\nabla} W), \quad (7)$$

where $W(x, y_1, \dots, y_{N-1}; t)$ is the distribution function, $\vec{J}(x, y_1, \dots, y_{N-1}; t)$ is the density of particle’s current, and the particle mass and Boltzmann constant are put to unity, $m = 1$ and $k_B = 1$.

For a steady state, Eq. (7) takes the form

$$T \frac{\partial W}{\partial x} + W \frac{\partial V_f}{\partial x} = -\eta J_x \quad (8)$$

for the x component, and a similar form for other degrees of freedom. The density \bar{J} of the current should satisfy the equation

$$\frac{\partial J_x}{\partial x} + \sum_{i=1}^N \frac{\partial J_{y_i}}{\partial y_i} = 0. \quad (9)$$

To reduce notations, below we consider the case of $N = 2$ only; generalization to the $N > 2$ case is trivial. Let us introduce the one-dimensional density and current as

$$\rho(x) = \int_{-\infty}^{+\infty} dy W(x, y), \quad (10)$$

$$j(x) = \int_{-\infty}^{+\infty} dy J_x(x, y). \quad (11)$$

Owing to the condition (5), the current $j(x)$ does not depend on x ,

$$\frac{dj(x)}{dx} = -J_y(x, +\infty) + J_y(x, -\infty) = 0, \quad (12)$$

where we have used Eq. (9). Thus, integrating both parts of Eq. (8) over y , we obtain the one-dimensional equation

$$T \frac{d\rho(x)}{dx} + \rho(x) \frac{dV_F(x)}{dx} = -\eta j, \quad (13)$$

where we introduced the potential $V_F(x)$ defined by the equation

$$\frac{dV_F(x)}{dx} = [\rho(x)]^{-1} \int_{-\infty}^{+\infty} dy W(x, y) \frac{\partial V_f(x, y)}{\partial x}. \quad (14)$$

Now, if $V_F(x)$ may be presented in the form

$$V_F(x) = V_N(x; f) - fx, \quad (15)$$

where $V_N(x; f)$ is a periodic function on x , Eq. (13) takes the form studied in [8], and the diffusion coefficient can be calculated as

$$D = D_f (I_+ I_-)^{-1}, \quad I_{\pm}(T) = (2\pi)^{-1} \int_0^{2\pi} dx e^{\pm V_{\text{eff}}(x)/T}, \quad (16)$$

where $D_f = T/\eta$ and $V_{\text{eff}}(x) = \lim_{f \rightarrow 0} V_N(x; f)$. Thus, the diffusion coefficient D is determined by the one-dimensional function $V_N(x; 0)$. In the limit $f \rightarrow 0$ we may substitute the equilibrium distribution function $W = W_{\text{eq}} \propto \exp(-V_N/T)$ into Eq. (14), thus obtaining

$$\frac{dV_{\text{eff}}(x)}{dx} = \frac{\int_{-\infty}^{+\infty} dy e^{-V_N(x, y)/T} \partial V_N(x, y)/\partial x}{\int_{-\infty}^{+\infty} dy e^{-V_N(x, y)/T}}. \quad (17)$$

Emphasize that this is the key approximation which is rigorous in the overdamped limit only. For the

underdamped case, $\eta \rightarrow 0$, a similar multiplicative separation in the Fokker-Planck-Kramers equation, $W(x, y, v_x, v_y, f) \propto W(x, v_x, f) W_{\text{eq}}(y, v_y)$, does not work even in the $f \rightarrow 0$ limit.

Let $V_N(x, y)$ has the form

$$V_N(x, y) = V(x) + U(y) + v(x, y), \quad (18)$$

where the function $v(x, y)$ describes the coupling between the two degrees of freedom. Then the effective potential $V_{\text{eff}}(x)$ can be presented in the following form,

$$V_{\text{eff}}(x) = V(x) - TS(x, T), \quad (19)$$

where the ‘‘entropy potential’’ $S(x, T)$ is defined by the expression

$$S(x, T) = \ln \int_{-\infty}^{+\infty} dy \exp\{-[U(y) + v(x, y)]/T\}. \quad (20)$$

Notice that $S(x)$ does not depend on $V(x)$.

III. APPLICATIONS

A. Pure entropy barriers

Let $V(x) = 0$ in Eq. (18),

$$U(y) = \frac{1}{2} m \omega_1^2 y^2, \quad (21)$$

and

$$v(x, y) = \frac{1}{4} m (\omega_2^2 - \omega_1^2) (1 - \cos x) y^2, \quad (22)$$

so that the atomic motion is inactivated in the x direction, but the frequency of transverse oscillation depends on x , $\omega = \omega_1$ at $x = 0$ and $\omega = \omega_2$ at $x = \pi$. Then the integral in Eq. (20) can be easily evaluated analytically, and the entropy potential is given by the expression

$$S(x) = -\frac{1}{2} \ln \left\{ 1 + \frac{1}{2} \left[\left(\frac{\omega_2}{\omega_1} \right)^2 - 1 \right] (1 - \cos x) \right\}. \quad (23)$$

Notice that the entropy potential (23) does not depend on temperature, because both potentials (21) and (22) depend on y in the same way ($\propto y^2$). The function $S(x)$ is shown in Fig. 1. It is periodic with the period $a = 2\pi$ and the height $\varepsilon_S = |\ln(\omega_2/\omega_1)|$. The diffusion coefficient is given by $D = D_f F$, where the entropy factor F depends on the ratio of frequencies $z = \omega_2/\omega_1$ only,

$$F(z) = [I_+(z) I_-(z)]^{-1}, \quad (24)$$

where

$$I_{\pm}(z) = \pi^{-1} \int_0^{\pi} dx \left[1 + \frac{1}{2} (z^2 - 1) (1 - \cos x) \right]^{\pm 1/2}. \quad (25)$$

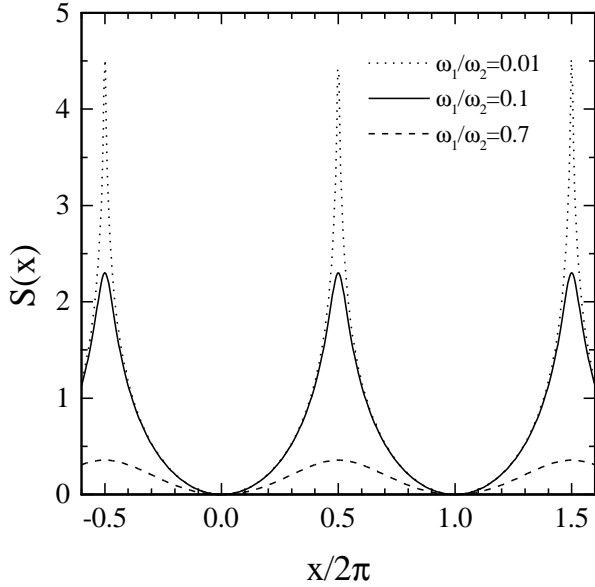


FIG. 1. The entropy potential $S(x)$ for pure entropic barriers with $\omega_1/\omega_2 = 0.01$ (dotted curve), $\omega_1/\omega_2 = 0.1$ (solid curve), and $\omega_1/\omega_2 = 0.7$ (dashed curve), respectively.

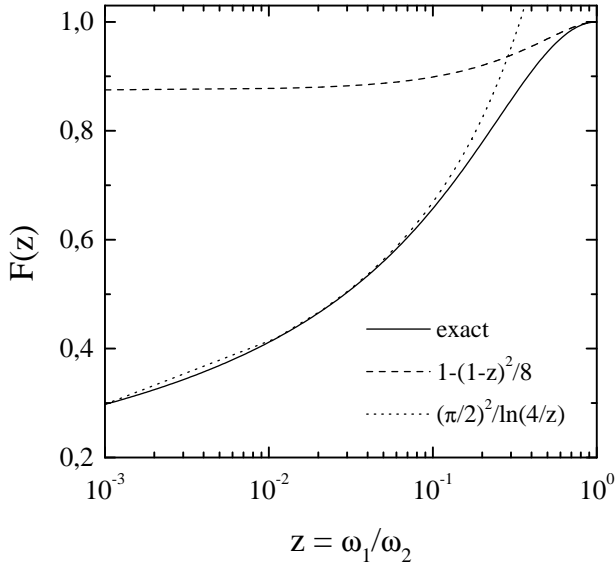


FIG. 2. The entropy factor $F(\omega_1/\omega_2)$ for pure entropy barriers in the overdamped limit.

Equations (24,25) yield $F(z) = (\pi/2)^2 \mathbf{K}^{-1}(\sqrt{1-z^2}) \mathbf{E}^{-1}(\sqrt{1-z^2})$, where \mathbf{K} is the complete elliptic integral of first kind. Near $z \approx 1$ the function $F(z)$ has the expansion $F(z) \approx 1 - \frac{1}{8}(1-z)^2$, while at $z \rightarrow 0$ it behaves as $F(z) \approx (\pi/2)^2 \ln^{-1}(4/z)$. The function $F(z)$ is presented in Fig. 2. One can see that in the overdamped limit, the effect of entropy barriers is not too strong, in particular, even for $\omega_1/\omega_2 = 0.1$ the diffusion coefficient

reduces comparing with the free-diffusion value by a factor of $F(0.1) \approx 0.66$ only. Indeed, although the height ε_S tends to infinity at $z \rightarrow 0$, the width of barriers becomes very narrow and thus cannot strongly modify the diffusion coefficient.

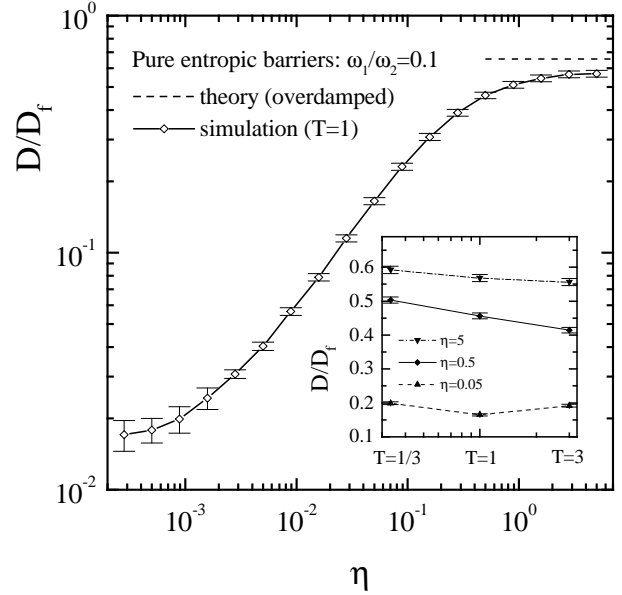


FIG. 3. The diffusion coefficient D/D_f (where $D_f = k_B T/m\eta$) as function of the friction coefficient η for pure entropic barriers with $\omega_1 = 0.1$ and $\omega_2 = 1$ at $T = 1$. Inset: dependence on temperature ($T = 1/3, 1$ and 3) for $\eta = 0.05$ (up triangles), 0.5 (diamonds) and 5 (down triangles).

In the underdamped case, on the contrary, the role of entropy barriers is essential. The dependence of the diffusion coefficient on the damping constant η was obtained numerically and shown in Fig. 3. One can see that the function $D(\eta)$ exhibits a typical behavior of activated diffusion ($D \propto \eta^{-1}$ at small and large frictions with a crossover between the limits) as might be expected from the shape of the entropy potential $S(x)$ of Fig. 1. In the overdamped limit the average jump length is equal to the period of the potential $S(x)$, $\lambda \approx 2\pi$, while in the underdamped limit long jumps with $\lambda/2\pi \gg 1$ play the dominant role as shown in Fig. 4 (in these simulations we assumed that the atom is trapped in a given well if it has sojourned in this well for a time lapse not shorter than $(2\eta)^{-1}$ [1,21]). The effect of entropy barriers is even stronger than might be expected from the analogy with the energy barriers of the same height. For example, for the frequencies $\omega_1/\omega_2 = 0.1$ used in the simulation, the height of the barrier is $\varepsilon_S = S(\pi) \approx 2.3$, that would give the ratio $D(\eta \rightarrow \infty)/D(\eta \rightarrow 0) \approx 2\varepsilon_S/k_B T \approx 4.6$ for the $T = 1$ case, while the simulation leads to the ratio $D(\eta \rightarrow \infty)/D(\eta \rightarrow 0) > 33$. From Fig. 4b one can see that $\langle \lambda/2\pi \rangle \approx 10^2$ for the case of $\eta = 10^{-3}$, while for the one-dimensional diffusion it should be $\langle \lambda/2\pi \rangle \sim \eta^{-1} =$

10^3 . Thus, multi-dimensional effects result in a strong reduction of jump's length in the underdamped limit which leads to a decrease of the diffusion coefficient comparing with the 1D motion. Note also that the dependence on temperature (shown in inset of Fig. 3) is almost negligible as has to be expected for the entropy potential.

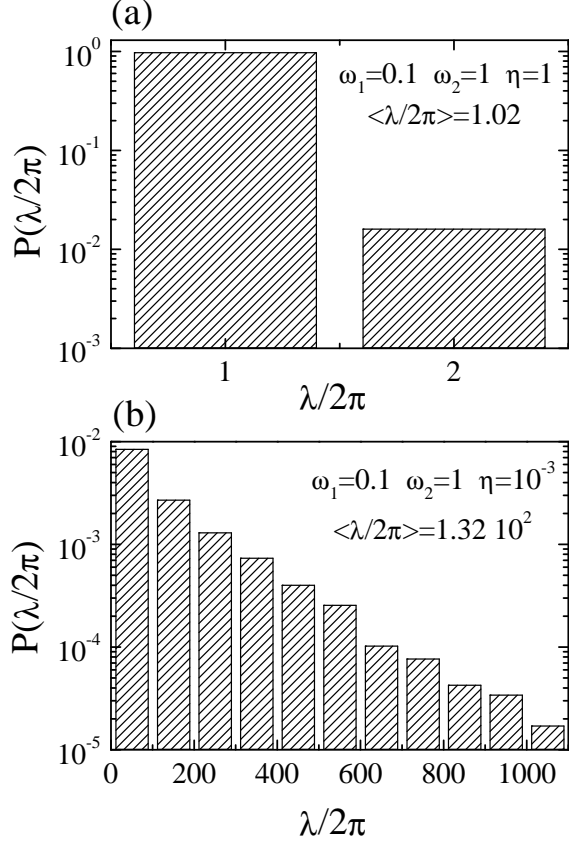


FIG. 4. Distribution of jump's length for pure entropic barriers with $\omega_1 = 0.1$ and $\omega_2 = 1$ at $T = 1$ for (a) overdamped case ($\eta = 1$) and (b) underdamped limit ($\eta = 10^{-3}$).

B. Atom in a corrugated channel

Let now the dependence of the external potential $V_N(x, y)$ on y is still given by Eqs. (21) and (22), but the motion in the x direction is activated,

$$V(x) = \frac{1}{2} \varepsilon (1 - \cos x), \quad (26)$$

where ε is the height of the external potential. At the minima of the potential (26) the transverse vibrations are characterized by the frequency ω_1 , while at the saddle points, by the frequency ω_2 . In the one-dimensional case, as well as for the 2D case with $\omega_1 = \omega_2$, in the overdamped limit we have, according to Eq. (1),

$D_{\text{Smoluchowski}} = D_f I_0^{-2}(\varepsilon/2T)$. Because the entropy potential $S(x)$ does not depend on the function $V(x)$, it is still given by Eq. (23), and the integral (16) can be easily evaluated. The results for the overdamped limit are shown in Fig. 5, which can be compared with the simulation results for different frictions presented in Figures 6 and 7.

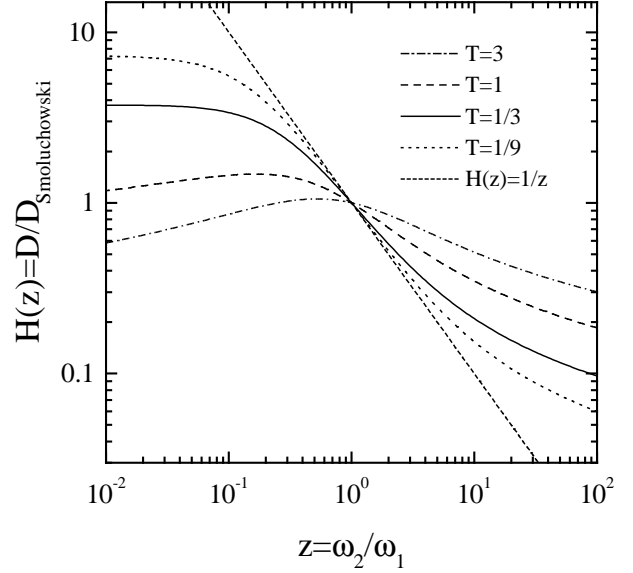


FIG. 5. Activated diffusion with the barrier $\varepsilon = 2$: D [normalized on the Smoluchowski value (1)] versus the ratio of transverse frequencies $z = \omega_2/\omega_1$ in the overdamped limit for the temperatures $T = 3$ (dot-dashed curve), $T = 1$ (dashed curve), $T = 1/3$ (solid curve), and $T = 1/9$ (dotted curve). The short-dashed line shows the TST approximation.

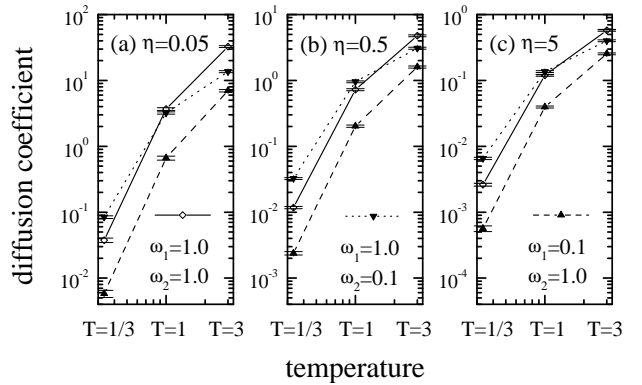


FIG. 6. D versus T for the activated motion with the barrier $\varepsilon = 2$ for three values of the transverse frequencies (open diamonds and solid curves for $\omega_1 = \omega_2 = 1.0$, down triangles and dotted curves for “wide barriers” with $\omega_1 = 1.0$ and $\omega_2 = 0.1$, and up triangles and dashed curves for “narrow barriers” with $\omega_1 = 0.1$ and $\omega_2 = 1.0$) for three values of the external damping: (a) $\eta = 0.05$, (b) $\eta = 0.5$, and (c) $\eta = 5$.

From the $D(T)$ dependence of Figures 5 and 6 one can see that at high temperatures, when the motion is in-activated, the $\omega_1 = \omega_2$ case leads to the maximum of the diffusion coefficient similarly to the case with pure entropic barriers. With temperature decreasing, the energy barriers and the entropy barriers play “in phase” for the “narrow-barriers” case of $\omega_1 < \omega_2$, and “in antiphase” for the “wide-barriers” case of $\omega_1 > \omega_2$. At low temperatures $D > D_{1D}$ for the case of $\omega_1 > \omega_2$ at high and moderate frictions in agreement with predictions of the TST approach. The effect, however, is smaller than the TST predicts: in simulation we found that the diffusion coefficient changes only in three times when the ratio of frequencies is equal to ten. At very low frictions (e.g., $\eta < 10^{-2}$ in Fig. 7), the entropy barriers become more important than the energy barriers, and the diffusion coefficient again becomes smaller than the 1D one for all cases of $\omega_1 \neq \omega_2$ as it was for the case of pure entropic barriers.

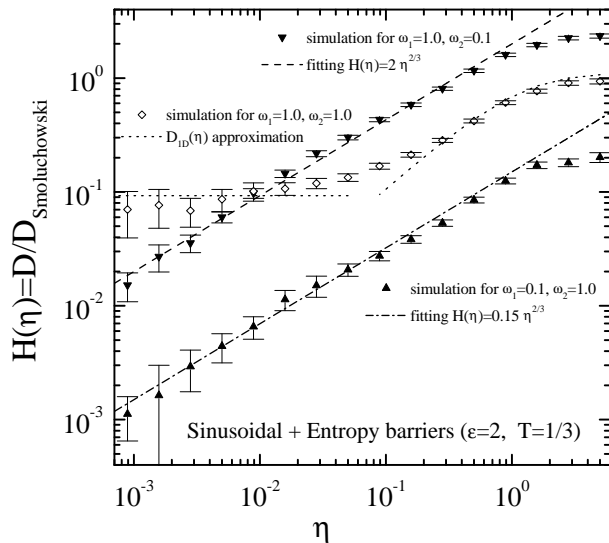


FIG. 7. The diffusion coefficient D [normalized on the Smoluchowski value (1)] as function of the friction coefficient η for the activated motion with the barrier $\varepsilon = 2$ at $T = 1/3$ for three values of the transverse frequencies: (a) $\omega_1 = \omega_2 = 1.0$ [open diamonds, the dotted curves show the 1D approximate values $D \approx (\omega_0/2\pi)Aa^2B(\eta)$ and $D \approx \pi D_f A/2$ at high and low frictions respectively], (b) $\omega_1 = 1.0$ and $\omega_2 = 0.1$ (down triangles, “wide barriers”), and (c) $\omega_1 = 0.1$ and $\omega_2 = 1.0$ (up triangles, “narrow barriers”). The dashed curves show the fit $D(\eta) \propto \eta^{-1/3}$.

For moderate and low frictions the simulation results of Fig. 7 can be fitted by a dependence $D(\eta) \propto \eta^{-1/3}$. Because the escape rate R is still proportional to η in the multi-dimensional case [22], we may conclude that in the present case, the average jump length scales as $\langle \lambda \rangle \propto \eta^{-2/3}$, which is in agreement with the results of pure entropic barriers presented in the previous subsection,

and also may be compared with the 1D law $\langle \lambda \rangle \propto \eta^{-1}$ and the 2D simulation result [18] $\langle \lambda \rangle \propto \eta^{-3/4}$. Thus, in the underdamped limit multi-dimensional effects lead to decreasing of diffusivity (comparing with the 1D case) due to reduction of jump length which scales as $\langle \lambda \rangle \propto \eta^{-2/3}$ instead of the 1D scaling law $\langle \lambda \rangle \propto \eta^{-1}$.

C. Diffusion of the dimer

Now we can study diffusion of a dimer in the 1D sinusoidal potential. Let x_1 and x_2 are the coordinates of two atoms coupled by the elastic spring with the constant g , and a_0 is the equilibrium distance ($0 \leq a_0 \leq \pi$). Then the Hamiltonian of the system takes the form

$$H = \frac{1}{2}m_a\dot{x}_1^2 + \frac{1}{2}m_a\dot{x}_2^2 + \frac{1}{2}\varepsilon_s(1 - \cos 2\pi x_1/a_s) + \frac{1}{2}\varepsilon_s(1 - \cos 2\pi x_2/a_s) + \frac{1}{2}g(x_2 - x_1 - a_0)^2. \quad (27)$$

In what follows we put $\varepsilon_s = 2$, $m_a = 1$, $a_s = 2\pi$, and in the present paper we consider the case of $a_0 = 0$ only. Introducing the coordinates $x = x_1 + x_2$ and $y = x_2 - x_1$, the Hamiltonian (27) can be rewritten as

$$H = \frac{1}{2}m(\dot{x}^2 + \dot{y}^2) + V_N(x, y), \quad (28)$$

$$V_N(x, y) = \frac{1}{2}\varepsilon \left(1 - \cos \frac{x}{2} \cos \frac{y}{2}\right) + \frac{1}{2}g y^2, \quad (29)$$

which describes the motion of one particle of mass $m = m_a/2 = 1/2$ in the x -periodic potential of height $\varepsilon = 2\varepsilon_a = 4$ and period $a = 2a_s = 4\pi$.

The adiabatic trajectory for this system was studied in [20]. Its shape depends on a value of the elastic constant g . The points $(x, y) = (4\pi n, 0)$, where n is an integer, always correspond to the absolute minimum of the potential energy. Near the minimum, the potential energy has the expansion $V_N(x, y) \approx \frac{1}{2}m(\omega_{0x}^2 x^2 + \omega_{0y}^2 y^2)$ with $\omega_{0x} = 1$ and $\omega_{0y} = (2g + 1)^{1/2}$. For a strong spring, $g \geq 1/2$, there is only one saddle point at $(x_s, y_s) = (2\pi, 0)$ between two adjacent minima $(0, 0)$ and $(4\pi, 0)$. Near the saddle, the potential energy has the expansion

$$V_N(x, y) \approx \varepsilon_s + \frac{1}{2}m[-\omega_{sx}^2(x - x_s)^2 + \omega_{sy}^2(y - y_s)^2] \quad (30)$$

with $\omega_{sx} = 1$ and $\omega_{sy} = (2g - 1)^{1/2}$, so that the activation energy for dimer motion is equal to $\varepsilon_s = \varepsilon = 4$ (see Fig. 8). Therefore, dimer diffusion can be approximately described as motion of one atom in the corrugated periodic potential with the transverse frequencies $\omega_{1,2} = (2g \pm 1)^{1/2}$, i.e. it corresponds to the case of “wide” barriers studied in the previous subsection. Thus, although the shape of adiabatic trajectory does not depend

on the elastic constant for the case of strong coupling, the diffusion coefficient does depend on g , it increases when $g \rightarrow 1/2$ due to decreasing of the transverse curvature at the saddle point. The simulation results of Fig. 9 show that the harmonic approximation describes the $D(g)$ dependence with a good accuracy. From Fig. 10, where the ratio $D(g)/D(0)$ is presented for different temperatures, one can see also that close to the critical point $g = 1/2$, when anharmonicity of transverse vibrations at the saddle point is large, the entropy factor strongly depends on T , especially at low temperatures.

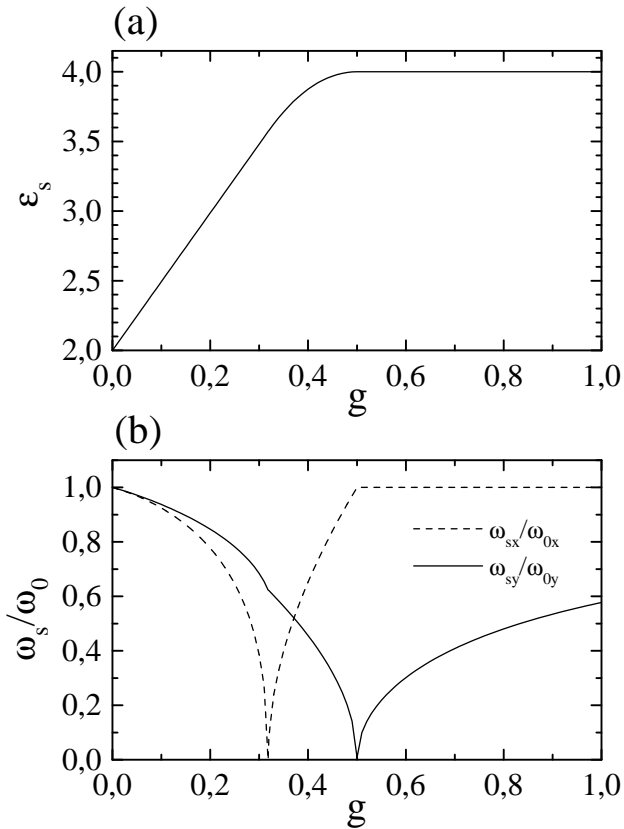


FIG. 8. (a) The activation energy ε_s and (b) the ratio of frequencies at the saddle and minimum points as functions of the elastic constant g for dimer's diffusion.

For intermediate values of the elastic constant, $1/\pi \leq g < 1/2$, the adiabatic trajectory still has only one saddle point $(2\pi, y_s)$ between the adjacent minima, where y_s is now a solution of the transcendental equation $\sin(y_s/2) = gy_s$. Near the saddle, the potential energy has the expansion (30) with the frequencies $\omega_{sx} = [1 - (gy_s)^2]^{1/4}$ and $\omega_{sy} = (2g - \omega_{sx}^2)^{1/2}$. The saddle is characterized by the energy $\varepsilon_s(g) = \frac{1}{2}\varepsilon [1 + \cos(y_s/2)] + \frac{1}{2}gy_s^2$, so that $2 + \pi/2 < \varepsilon_s < 4$.

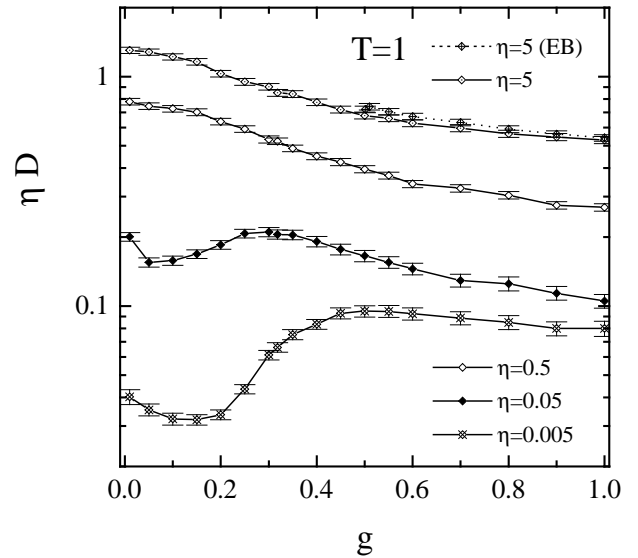


FIG. 9. The dependence of the diffusion coefficient D (times η) on the elastic constant g at $T = 1$ for different values of the damping constant: $\eta = 5$ (dotted diamonds), $\eta = 0.5$ (open diamonds), $\eta = 0.05$ (solid diamonds), and $\eta = 0.005$ (crossed diamonds). The dotted curve and plussed diamonds show the simulation results for the “atom in channel” model with $\eta = 5$ and other parameters adjusted to the dimer case.

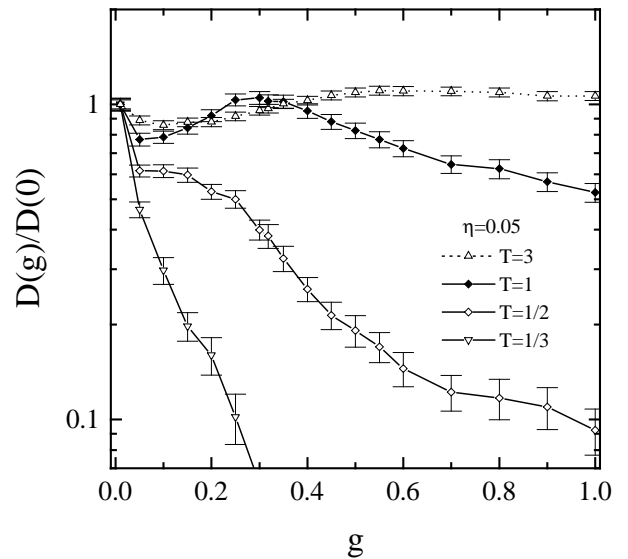


FIG. 10. The ratio $D(g)/D(0)$ as function of the elastic constant g for the dimer diffusion at $\eta = 0.05$ and different temperatures $T = 3, 1, 1/2$, and $1/3$.

Finally, for a weak coupling between dimer's atoms, $g < 1/\pi$, there are two saddle points between the adjacent minima $(0, 0)$ and $(4\pi, 0)$, with a local minimum of the potential energy between these saddle points. The coordinates of the saddle points are $(2\pi - x', \pi)$ and

$(2\pi + x', \pi)$, where $x' = 2 \cos^{-1}(g\pi)$. These saddle points are characterized by the energy $\varepsilon_s(g) = \frac{1}{2}(\varepsilon + g\pi^2)$, so that $2 < \varepsilon_s < 2 + \pi/2$. Near the saddle, the potential energy has the expansion (30) with coefficients $\omega_{sx} = (g - G)^{1/2}$ and $\omega_{sy} = (g + G)^{1/2}$, where $G = [1 - (\pi^2 - 1)g^2]^{1/2}$.

The whole dependence $\varepsilon_s(g)$ is shown in Fig. 8a. The activation energy monotonically increases from the single-atom value $\varepsilon_s = 2$ at $g = 0$ to the rigid-dimer value $\varepsilon_s = 4$ at $g = 1/2$ and then remains constant. Thus, one could expect that the diffusion coefficient should monotonically decrease with g increasing. However, the simulation results of Fig. 10 show that often this is not true. The peculiarity in the transverse frequencies at the point $g = 1/2$, where the saddle transverse frequency reaches zero, leads to a maximum of the function $D(g)$ close to this point, if the damping is small, $\eta \lesssim 0.5$, and the temperature is not too low, $T \gtrsim 1$ (recall $\varepsilon = 4$). Thus, multi-dimensional effects may strongly affect dimer's diffusivity.

IV. CONCLUSION

In the present paper we studied in details the diffusion of a particle in two-dimensional space which is periodic along x and unbounded in the transverse direction. We calculated the entropy factor which emerges due to transverse degree of freedom, both in the overdamped limit (analytically) and in the underdamped case (numerically), and compared it with the prediction of the transition-state theory. We showed that in the underdamped limit, the multi-dimensional effects lead to reduction (comparing with the one-dimensional motion) of jump lengths between subsequent trapping of the atom in bottoms of the external periodic potential. The simulation predicts that jump lengths scale as $\langle \lambda \rangle / \langle \lambda_{1D} \rangle \propto \eta^{1/3}$. This leads to a decrease of diffusivity which now scales as $D \propto \eta^{-1/3}$ instead of the 1D dependence $D_{1D} \propto \eta^{-1}$.

In the overdamped limit, the entropy factor (and, therefore, the prefactor in the Arrhenius formula for activated diffusion) does not depend on temperature as long as the transverse motion near the adiabatic trajectory may be described by the harmonic approximation. Simulation shows that this remains true, at least approximately, for low damping as well. Thus, in most cases the experimentally observed dependence of the prefactor on temperature has to be attributed to collective effects due to interaction between diffusing particles or/and between the atom and (deformable) substrate. However, in the case of dimer diffusion at some value of the interaction between the atoms, when the saddle transverse frequency is equal zero, the anharmonicity of the transverse potential begins to play the important role and the entropy factor strongly depends on T .

ACKNOWLEDGMENTS

Helpful discussions with T. P. Valkering are gratefully acknowledged. This work was partially supported by the INTAS Grant 97-31061.

* Electronic address: obraun@iop.kiev.ua

- [1] H. Risken, *The Fokker-Planck Equation* (Springer, Berlin, 1996).
- [2] P. Hänggi, P. Talkner, and M. Borkovec, *Rev. Mod. Phys.* **62**, 251 (1990).
- [3] V. I. Mel'nikov, *Phys. Rep.* **209**, 1 (1991).
- [4] A. G. Naumovets and Yu. S. Vedula, *Surf. Sci. Repts.* **4**, 365 (1985); R. Gomer, *Rep. Prog. Phys.* **53**, 917 (1990).
- [5] B. S. Swartzentruber, *Phys. Rev. Lett.* **76**, 459 (1996); W. Wulfhekel, B. J. Hattink, H. J. Zandvliet, G. Rosenfeld, and B. Poelsema, *Phys. Rev. Lett.* **79**, 24949 (1997); E. Zoethout, H. J. Zandvliet, W. Wulfhekel, G. Rosenfeld, and B. Poelsema, *Phys. Rev. B* **58**, 16167 (1998); H. J. Zandvliet, T. M. Galea, E. Zoethout, and B. Poelsema, *Phys. Rev. Lett.* **84**, 1523 (2000).
- [6] S. C. Wang and G. Ehrlich, *Surf. Sci.* **239**, 301 (1990); G. L. Kellogg, *Appl. Surf. Sci.* **67**, 134 (1993); S. C. Wang and G. Ehrlich, *Phys. Rev. Lett.* **79**, 4234 (1997); S. C. Wang, U. Kurpick, and G. Ehrlich, *Phys. Rev. Lett.* **81**, 423 (1998).
- [7] A. F. Voter, *Phys. Rev. B* **34**, 6819 (1986); C.-L. Liu and J. B. Adams, *Surf. Sci.* **268**, 73 (1992); C. Massobrio and P. Blandin, *Phys. Rev. B* **47**, 13 687 (1993); J. C. Hamilton, M. S. Daw, and S. M. Foiles, *Phys. Rev. Lett.* **74**, 2760 (1995); Clinton DeW. Van Siclen, *Phys. Rev. Lett.* **75**, 1574 (1995); S. V. Khare, N. C. Bartelt, and T. L. Einstein, *Phys. Rev. Lett.* **75**, 2148 (1995); D. S. Sholl and R. T. Skodje, *Phys. Rev. Lett.* **75**, 3158 (1995).
- [8] R. L. Stratonovich, *Topics in the Theory of Random Noise* (Gordon and Breach, New York, 1967); Yu. M. Ivanchenko and L. A. Zil'berman, *JETP Lett.* **8**, 113 (1968) [*Sov. Phys. JETP* **28**, 1272 (1969)]; V. Ambe-gaokar and B. I. Halperin, *Phys. Rev. Lett.* **22**, 1364 (1969).
- [9] S. Glasstone, K. J. Laidler, and H. Eyring, *The Theory of Rate Processes* (McGraw-Hill, New York, 1941).
- [10] H. A. Kramers, *Physica* **7**, 284 (1940).
- [11] J. W. M. Frenken, B. J. Hinch, J. P. Toennies, and Ch. Wöll, *Phys. Rev. B* **41**, 938 (1990); G. Ehrlich, *Surf. Sci.* **246**, 1 (1991); E. Ganz, S. K. Theiss, I. S. Hwang, J. Golovchenko, *Phys. Rev. Lett.* **68**, 1567 (1992); J. Ellis and J. P. Toennies, *Phys. Rev. Lett.* **70**, 2118 (1993); D. C. Senft and G. Ehrlich, *Phys. Rev. Lett.* **74**, 294 (1995).
- [12] V. I. Mel'nikov and S. V. Meshkov, *J. Chem. Phys.* **85**, 1018 (1986).
- [13] R. Ferrando, R. Spadacini, and G. E. Tommei, *Phys. Rev. A* **46**, R699 (1992).
- [14] R. Ferrando, R. Spadacini, and G. E. Tommei, *Phys. Rev. E* **51**, 126 (1995).

- [15] G. H. Vineyard, J. Phys. Chem. Solids **3**, 121 (1957).
- [16] V. P. Zhdanov, Surf. Sci. **214**, 289 (1989).
- [17] K. Haug, G. Wahnström, and H. Metiu, J. Chem. Phys. **90**, 540 (1989); **92**, 2083 (1990).
- [18] L. Y. Chen, M. R. Baldan, and S. C. Ying, Phys. Rev. B **54**, 8856 (1996).
- [19] H. D. Vollmer, Z. Physik B **33**, 103 (1979).
- [20] O. M. Braun, Surf. Sci. **230**, 262 (1990).
- [21] M. Borromeo and F. Marchesoni, Phys. Rev. Lett. **84**, 203 (2000).
- [22] M. Borkovec and B. J. Berne, J. Chem. Phys. **82**, 794 (1985); J. Chem. Phys. **84**, 4327 (1986); J. Chem. Phys. **86**, 2444 (1987); J. E. Straub, M. Borkovec, and B. J. Berne, J. Chem. Phys. **86**, 4296 (1987).